NACA TN No. 1594

NATIONAL ADVISORY COMMITTEE FOR AERONAUTICS

TECHNICAL NOTE

No. 1594

EXPERIMENTAL INVESTIGATION OF THE EFFECTS OF CONCENTRATED WEIGHTS ON FLUTTER CHARACTERISTICS OF A STRAIGHT CANTILEVER WING

By Harry L. Runyan and John L. Sewall

Langley Memorial Aeronautical Laboratory
Langley Field, Va.

Washington
June 1948

NATIONAL ADVISORY COMMITTEE FOR AERONAUTICS

TECHNICAL NOTE NO. 1594

EXPERIMENTAL INVESTIGATION OF THE EFFECTS OF CONCENTRATED WEIGHTS ON FLUTTER CHARACTERISTICS OF A STRAIGHT CANTILEVER WING

By Harry L. Runyan and John L. Sewall

SUMMARY

Results are presented to show the effects on the flutter characteristics of mounting concentrated weights at various positions on an untapered wing model. The model was mounted as a rigid cantilever and was tested with concentrated weights that were 38, 60, 90, and 100 percent of the wing weight. The moment of inertia, the chordwise position of the weight, and the spanwise position of the weight were varied. In several tests, an end plate was used, which was believed to change the aerodynamic aspect ratio of the wing. The effects of these variations on the flutter characteristics are presented in a form which may be conventiently used for correlation with theoretical results.

INTRODUCTION

Airplane design trends are leading to the placement of heavy concentrated masses on the outer wing panels and sometimes on the wing tip. Present-day flutter analysis is based on many simplifying assumptions and, with the inclusion of these concentrated masses into the problem, the analytical solution is at best approximate. Experimental verification of these simplifying assumptions is needed for more accurate design criterions. The purpose of this paper is therefore to present a consistent series of flutter tests made on a simplified structure in order that the assumptions made in the various fundamental analyses may be evaluated.

Dynamically similar models of full-scale airplanes are sometimes used for flutter testing, but the production of such models is exceedingly difficult. For this reason simplified models that could be built, tested, and analyzed more easily are being used to study the assumptions in the theoretical analysis. The model wing used for this series of tests was a straight, untapered, cantilever wing having uniform properties the entire length of the wing. Concentrated weights differing in mass and moment of inertia were moved chordwise and spanwise on the wing. Because of the simplicity of construction of the model, no attempt has been made to indicate the most favorable location for a concentrated weight from

considerations of the flutter characteristics of an actual wing. In order to obtain further information about the character of the air forces, an unattached end plate was installed at the tip for a few tests. The effect of the end plate was to increase the aerodynamic aspect ratio.

The flutter tests presented herein were made in the 4.5-foot flutter tunnel on a single model and required almost 100 separate runs. The model did not change its properties throughout the program.

SYMBOLS

W	weight of wing model, pounds
W_w	weight of concentrated weight, pounds
l	length of wing model, feet
b	half chord of wing model, feet
I_w	mass moment of inertia of weight about wing elastic axis, inch-pound-second^2
I_{CG}	mass moment of inertia of wing about center of gravity, inch-pound-second^2
I_{EA}	mass moment of inertia of wing about elastic axis, inch-pound-second^2
EI	bending rigidity of wing, pound-inches^2
GJ	torsional rigidity of wing, pound-inches^2
ρ	density of testing medium, slugs per cubic foot
m	mass of wing per unit length
κ	mass ratio $\left(\frac{\pi\rho b^2}{m}\right)$
r_α	nondimensional radius of gyration relative to elastic axis $\left(\sqrt{\frac{I_{EA}}{12\,lmb^2}}\right)$
e_w	distance between elastic axis of wing and center of gravity of weight referred to half chord
f_{h_1}	natural first bending frequency at zero airspeed, cycles per second
f_{h_2}	natural second bending frequency at zero airspeed, cycles per second

f_t natural first torsional frequency at zero airspeed, cycles per second

f_f flutter frequency, cycles per second

V_i indicated airspeed at flutter, feet per second

V true airspeed at flutter, feet per second

ω_t angular natural first torsional frequency at zero airspeed, radians per second $(2\pi f_t)$

ω_f angular flutter frequency, radians per second $(2\pi f_f)$

$\frac{V}{b\omega_t}$ nondimensional reference flutter-velocity coefficient

$\frac{V}{b\omega_f}$ reduced wave length at flutter

ω_{h_1} angular natural first bending frequency at zero airspeed, radians per second $\left(2\pi f_{h_1}\right)$

ω_{h_2} angular natural second bending frequency at zero airspeed, radians per second $\left(2\pi f_{h_2}\right)$

Subscript:

w refers to the corresponding properties or parameters of the concentrated weights

APPARATUS

The Langley 4.5-foot flutter research tunnel was used for this series of tests. This tunnel is unusual in that the testing medium used may be either air or Freon-12 or any mixture of the two at any pressure from 30 inches of mercury to 4.3 inches of mercury, absolute. Utilizing this feature makes it possible to vary the mass ratio κ, Mach number, and Reynolds number (each independently) for a given wing over a large range of values.

The model wing, built of balsa wood with a duralumin insert, had a 48-inch length and an 8-inch chord and was mounted vertically as a

rigid cantilever from the top of the test section as shown in figure 1. This type of mounting resulted in symmetrical flutter or a flutter involving no bending or torsional deflections of the root. A cross-sectional view of the wing is given in figure 2 and the wing properties were as follows:

Chord, inches	8
Length, inches	48
Aspect ratio (geometric)	6
Taper ratio	1
Airfoil section	NACA 16010
W, pounds	3.48
I_{CG}, inch-pound-second^2	0.0382
I_{EA}, inch-pound-second^2	0.0384
EI, pound-inches^2	$.0.1407 \times 10^6$
GJ, pound-inches^2	0.0692×10^6
r_α^2	0.266
$\frac{1}{\kappa}$ (standard air, no weight)	32.6

The bending rigidity and torsional rigidity were determined experimentally from the static deflection curves of the wing in bending and torsion.

Weights which were approximately 38, 60, 90, and 100 percent of the wing weight (fig. 3) were used and the weight parameters (ratio of mass of weight to wing mass, distance of weight center of gravity from wing center of gravity in percent of the half chord, and the ratio of the polar moments of inertia) are given in table I.

The variation of weight 7 from 7a to 7f (fig. 3(g)) was obtained by moving the same weight chordwise on the weight support. This procedure resulted in maintaining the weight for all tests with weight 7 essentially constant while changing the mass moment of inertia about the wing elastic axis and the chordwise position of the center of gravity.

A high-speed motion-picture camera that was used to record the oscillations of the wing during flutter was situated outside the tunnel for ease of access as shown in figure 4. The camera had a film speed of 120 frames per second. Two examples of pictures taken with this camera are shown in figure 5. It is interesting to note the change in the shape of the flutter mode between the two cases, where the one case has a tip weight (weight 6, run 35; see table II) and the other a weight close to the midspan (weight 5, run 31; see table II).

Vibration records of the bending and torsional oscillations of the wing during flutter were obtained electrically by the use of strain gages mounted on the wing as shown in figure 1. The white squares indicate

bending gages and the circles indicate torsional gages. The strain gages feed through a system of bridges and amplifiers to a recording oscillograph.

The installation of the unattached end plate is shown in figure 6. The plate was so adjusted that the clearance between the plate and the wing was small in order to reduce as much as possible any air flow around the wing tip. With this installation, the aerodynamic aspect ratio was believed to be increased. In order to prevent destruction of the wing as a result of divergence, restraining wires were attached from the tunnel walls to the wing quarter chord at the tip. These wires had sufficient slack in them to permit adequate amplitude in flutter but still to save the wing when divergence occurred.

TEST PROCEDURE

Since flutter is a destructive phenomenon, recognition of flutter, recording the necessary data, and reduction of the airspeed must be accomplished in a very short interval of time to prevent damage to the model. Increases in the airspeed during the run were made slowly and, at speeds close to the point of flutter, airspeed increments of the order of one mile per hour were necessary. When flutter occurred, the recording oscillograph and movie camera were operated and the tunnel conditions were observed and recorded as shown in table II. For most runs, the natural frequencies were tabulated both before and after the actual run to determine whether the wing had been damaged by flutter. The remarks in table II regarding the flutter characteristics are based almost entirely on visual observations made at the time of the run and since the observer, because of the sudden and violent occurence of flutter, was principally concerned with saving the model, these remarks are inclined to be arbitrary.

RESULTS

The results of this investigation are presented to show the effect on flutter parameters of spanwise and chordwise variation of concentrated weights over the wing (figs. 7 to 26). In all plots, the various flutter parameters are presented as functions of the spanwise position of the concentrated weight from root to tip, with individual curves representing distinct chordwise weight positions. The flutter parameters are given as ratios of values obtained with concentrated weights at a given location to similar values obtained with the unweighted wing.

Examination of the flutter-speed ratio (figs. 7 and 8) reveals a general reduction followed by an increase in flutter speed for all

chordwise weight positions as the spanwise positions varied from root to tip. However, for weights located forward of the wing center of gravity (weights 4 and 6 in fig. 7; weights 7a, 7b, 7c in fig. 8), a divergence region was found which was a function of the mass of the weight and its chordwise location. The more forward the weight center of gravity and the greater the mass, the wider the divergence region. With the exception of weight 7c, flutter occurred with each of these forward weights located at the tip but appeared to approximate a second bending mode; whereas, for the inboard positions of these weights, the flutter mode was closer to a first bending mode.

For weights located rearward of the wing center of gravity (weight 5 in fig. 7 and weight 7f in fig. 8), flutter was obtained at all spanwise positions with no change in flutter mode evident at any point. Of special interest regarding these rearward weight positions is the reduction that they caused in the flutter speed.

The dotted curve in figure 7 shows the effects of the end-plate installation on the flutter-speed ratio for weight 6. With this plate in the tunnel the flutter speed dropped 5 percent for the unweighted wing and 15 percent for the wing with weight 6 at the 43-percent-span position. With the weight at the tip the flutter speed was reduced 6 percent but a more interesting phenomena than this reduction was the shift in flutter mode resulting from the presence of the plate. Figures 9 and 10 are parts of the oscillograph records taken during flutter. In figure 9, the bending traces are seen to be approximately 180° out of phase, whereas in figure 10 they are approximately in phase. An examination of the records of the natural frequencies at zero airspeed indicated that, when first bending was excited, the bending traces were approximately 180° out of phase and that, when second bending was excited, they were approximately in phase. Thus, comparison of the records in figures 9 and 10 with the records of the natural frequencies at zero airspeed shows that, with the end plate installed in the tunnel, there was a first bending mode in the flutter record and that, without the end plate, a second bending mode was evident in the flutter record. No appreciable change in the flutter frequency occurred with or without the addition of the end plate.

The variations of flutter-velocity coefficient $\frac{V}{b\omega_t}$ with reduced wave length $\frac{V}{b\omega_f}$ for all weight positions are shown in figures 11 to 14.

The natural torsional- and flutter-frequency ratios for all weight positions are given in figures 15 to 18. Of interest are the different shapes in the flutter-frequency curves for weight 6 in figure 16 and weight 7b in figure 18 compared with those of the other weight positions.

First and second bending-frequency ratios are given for all weight positions in figures 19 to 22. The general rise in the second bending curves occurred in the vicinity of the second bending node of the unweighted wing.

Curves of the ratio of first-bending frequency to torsion frequency and second-bending frequency to torsion frequency are given in figures 23 to 26. Of interest is the sharp difference in the shapes of the curves for both forward and rearward weight positions (weights 5 and 6 in figures 23 and 24; weights 7a and 7f in figures 25 and 26). No curves are given to show the effect of the end plate on the natural frequency in figures 19 to 26 because this effect was negligible.

CONCLUDING REMARKS

The results have been presented of almost 100 flutter tests in which concentrated weights were mounted rigidly to a straight cantilever wing. The moment of inertia and mass of the weights were varied and the weight position was varied chordwise and spanwise. During the entire series of flutter tests the elastic properties of the wing did not materially change. The results were presented in the form of curves that show the effects of varying concentrated weights on the various flutter parameters.

At the present time there exist several analytical methods of approach to the problem of flutter in wings with concentrated weights. The flutter data presented provide information from which the validity of these procedures may be evaluated by comparison with experimental results.

Langley Memorial Aeronautical Laboratory
National Advisory Committee for Aeronautics
Langley Field, Va., November 19, 1947

TABLE I

CONCENTRATED WEIGHT CHARACTERISTICS

Weight	$\frac{W_w}{W}$	e_w (a)	$\frac{I_w}{I_{EA}}$
1	0.636	0.039	1.40
2	.625	.039	.883
3	.375	−.050	.514
4	.636	−.625	1.91
5	.636	.687	2.68
6	1.040	−.937	7.50
7a	.917	−.818	4.26
7b	.931	−.578	2.86
7c	.940	−.360	2.04
7d	.946	−.140	1.555
7e	.954	.034	1.56
7f	.917	.500	2.27

[a] Negative values indicate concentrated weight locations forward of wing elastic axis.

TABLE II.- EXPERIMENTAL DATA

Run	Weight	Spanwise position (in. from root)	V_i (fps)	Percentage of Freon-12	Mach number	Reynolds number	V (fps)	ρ (slug/cu ft)	f_{h_1} (cps)	f_{h_2} (cps)	f_t (cps)	f_f (cps)	Remarks
1	1	47 (tip)	0	0	0	0 $\times 10^6$	0	-----	3.58	32.2	21.7	---	Fluttered in first bending mode with 2-inch amplitude at tip.
	1	47 (tip)	353	96.6	0.3992	4.043	191.4	0.008129	---	---	---	10.6	
	1	47 (tip)	0	0	0	0	0	-----	3.56	31.36	21.1	---	
2	1	36½	0	0	0	0	0	-----	4.46	39.2	24.33	---	Fluttered in first bending mode with strong torsion response and 1-inch amplitude at tip; torsion node forward of 50 percent chord
	1	36½	320	95.0	0.3556	3.754	171.4	0.008274	---	---	---	15.95	
	1	36½	0	0	0	0	0	-----	4.43	39.2	24.26	---	
3	1	29	0	0	0	0	0	-----	5.22	32.67	25.79	---	Fluttered in first bending mode with torsion node along leading edge;
	1	29	299	95.0	0.3278	3.506	159.3	0.008386	---	---	---	18.15	
	1	29	0	0	0	0	0	-----	5.22	32.67	25.57	---	
4	1	11	0	0	0	0	0	-----	6.41	30.67	37.3	---	Fluttered in second bending mode with node 15 inches from tip and 1-inch amplitude on trailing edge at tip.
	1	11	383	91.5	0.3418	3.760	170.6	0.008551	---	---	---	25.20	
	1	11	0	0	0	0	0	-----	6.32	31.04	37.1	---	
5	None	-----	0	0	0	0	0	-----	6.45	39.20	47.3	---	Fluttered in first bending mode with strong torsion response and 2-inch amplitude on trailing edge at tip
	None	-----	359	90.8	0.3651	3.955	181.8	0.008256	---	---	---	25.20	
	None	-----	0	0	0	0	0	-----	6.43	39.20	47.57	---	
6	2	47 (tip)	0	0	0	0	0	-----	3.61	30.63	29.4	---	Flutter involved both first and second bending modes with ½-inch amplitude on leading edge at tip; node 15 inches to 18 inches from tip.
	2	47 (tip)	364	89.5	0.3858	4.144	193.3	0.008440	---	---	---	10.47	
	2	47 (tip)	0	0	0	0	0	-----	3.61	30.15	29.4	---	
7	2	36½	0	0	0	0	0	-----	4.49	39.20	28.51	---	Fluttered in first bending with 1½-inch amplitude on trailing edge at tip; leading edge from tip to weight broke away; model repaired and used again.
	2	36½	336	88.8	0.3547	3.776	178.0	0.008466	---	---	---	15.89	
	2	36½	0	0	0	0	0	-----	4.52	39.20	29.04	---	
8	2	29	0	0	0	0	0	-----	5.21	31.36	30.49	---	Fluttered in first bending mode with 1-inch amplitude at tip.
	2	29	315	87.1	0.3302	3.491	168.4	0.008314	---	---	---	19.6	
	2	29	0	0	0	0	0	-----	5.21	32.07	30.15	---	
9	2	11	0	0	0	0	0	-----	6.98	30.95	40.83	---	Fluttered in first bending mode with 1-inch amplitude at tip.
	2	11	321	86.3	0.3370	3.512	172.9	0.008214	---	---	---	25.79	
	2	11	0	0	0	0	0	-----	6.41	30.95	40.09	---	
10	3	29	0	0	0	0	0	-----	5.62	33.69	35.39	---	Fluttered in first bending mode; no oscillograph record obtained at flutter point.
	3	29	324	87.2	0.3387	3.573	173.4	0.008313	---	---	---	No record	
	3	29	0	0	0	0	0	-----	---	---	---	---	
11	4	29	0	0	0	0	0	-----	5.22	35.10	24.5	---	No flutter; divergence
	4	29	376	86.2	0.4110	4.088	208.0	0.007775	---	---	---	0	
	4	29	0	0	0	0	0	-----	5.30	36.11	24.5	---	
12	4	11	0	0	0	0	0	-----	6.64	30.41	40.00	---	Fluttered in first bending mode with ½-inch tip amplitude
	4	11	330	86.1	0.3550	3.601	180.7	0.007933	---	---	---	22.84	
	4	11	0	0	0	0	0	-----	6.64	30.15	40.21	---	
13	4	47 (tip)	0	0	0	0	0	-----	3.65	34.35	22.5	---	Fluttered in second bending mode with node about 4 inches from tip.
	4	47 (tip)	345	85.9	0.3723	3.727	189.9	0.007857	---	---	Not clear	28.0	
	4	47 (tip)	0	0	0	0	0	-----	3.68	34.25	---	---	
14	4	41	0	0	0	0	0	-----	4.17	38.50	23.9	---	No flutter; divergence
	4	41	372	85.5	0.401	3.945	206	0.007750	---	---	---	0	
	4	41	0	0	0	0	0	-----	4.17	38.3	23.9	---	
15	4	20¾	0	0	0	0	0	-----	6.14	35.6	35.6	---	Fluttered in first bending mode.
	4	20½	368	85.3	0.3968	3.893	204.7	0.007718	---	---	---	19.0	
	4	20¼	0	0	0	0	0	-----	6.15	Not clear	35.6	---	
16	4	29	0	0	0	0	0	-----	5.18	34.77	24.74	---	No flutter; divergence.
	4	29	393	84.5	0.428	4.212	219	0.007675	---	---	---	0	
	4	29	0	0	0	0	0	-----	5.26	35.00	24.63	---	
17	4	26	0	0	0	0	0	-----	5.56	33.69	24.77	---	No flutter; divergence.
	4	26	404	84.3	0.432	4.400	221	0.007939	---	---	---	0	
	4	26	0	0	0	0	0	-----	5.54	34.00	22.91	---	

TABLE II.- EXPERIMENTAL DATA -- Continued

Run	Weight number	Spanwise position (in. from root)	V_i (fps)	Percentage of Freon-12	Mach number	Reynolds number	V (fps)	ρ (slug/cu ft)	f_{h_1} (cps)	f_{h_2} (cps)	f_t (cps)	f_f (cps)	Remarks
18	4 4 4	44 44 44	0 394 0	0 84.3 0	0 .427 0	0 4.188 $\times 10^6$ 0	0 220 0	------ 0.007675 ------	3.86 --- 3.86	35.83 --- 36.00	Not clear --- 23.59	--- 0 ---	No flutter; divergence
19	4 4 4	47 (tip) 47 (tip) 47 (tip)	0 340 0	0 84.3 0	0 .3647 0	0 3.668 0	0 188 0	------ .007851 ------	3.59 --- 3.62	33.13 --- 33.74	20.63 --- 22.6	--- 27.2 ---	Fluttered in second bending mode with node 3 inches from tip; amplitude $\frac{3}{8}$-inch on leading edge, 1 inch on trailing edge about 94 inches from root.
20	4 4	44 44	0 371	0 83.2	0 .426	0 3.706	0 219.5	------ .006907	3.83 ---	35.8 ---	23.38 ---	--- 0	No flutter; divergence
21	4 4	44 44	0 390	0 85.7	0 .511	0 3.382	0 264	------ .005233	3.80 ---	35.64 ---	23.33 ---	--- 0	No flutter; divergence
22	4	44	388	83.7	.553	3.165	283.5	.004471	---	---	---	0	No flutter; divergence
23	4 4	44 44	376 0	83.7 0	.591 0	2.729 0	304 0	.003620 ------	3.84 ---	35.83 ---	23.29 ---	@ ---	No flutter; divergence
24	4 4 4	47 (tip) 47 (tip) 47 (tip)	0 296 0	0 82.6 0	0 .507 0	0 1.972 0	0 262.5 0	------ .003043 ------	3.59 --- 3.61	33.74 --- 34.09	22.02 --- 22.83	--- 26.8 ---	Fluttered in second bending mode.
25	4 4	44 44	0 352	0 83.0	0 .7435	0 1.905	0 383.3	------ .002008	3.87 ---	36.35 ---	23.52 ---	--- 0	No flutter; divergence
26	4	44	327	78.2	.732	1.609	386	.001708	---	---	---	---	No flutter; divergence
27	5 5	47 (tip) 47 (tip)	0 252	0 6	0 .2284	0 1.042	0 257.7	------ .00229	3.53 ---	30.63 ---	20.36 ---	--- 8.71	Fluttered in first bending mode with $2\frac{1}{2}$-inch tip amplitude
28	5 5	41 41	0 247	0 0	0 .2234	0 1.020	0 252	------ .002285	4.08 ---	35.28 ---	21.51 ---	--- 10.8	Fluttered in first bending mode with 2-inch tip amplitude
29	5 5	37 37	0 242	0 0	0 .2186	0 .9914	0 247	------ .002282	4.32 ---	37.17 ---	22.13 ---	--- 12.56	Fluttered in first bending mode with 2-inch tip amplitude
30	5 5	29 29	0 230	0 0	0 .2080	0 .9427	0 235.5	------ .002281	5.03 ---	33.69 ---	22.27 ---	--- 14.29	Fluttered in first bending mode with $1\frac{1}{2}$-inch tip amplitude
31	5 5	26 26	0 234.5	0 0	0 .2120	0 .9614	0 240	------ .002281	5.16 ---	32.0 ---	21.78 ---	--- 14.0	Fluttered in first bending mode with 5-inch tip amplitude
32	5 5	18 18	0 243	0 0	0 .2200	0 .9927	0 248.5	------ .002272	6.19 ---	Not clear ---	21.90 ---	--- 16.06	Fluttered in first bending mode with 8-inch tip amplitude
33	5 5	11 11	0 288	0 0	0 .2624	0 1.169	0 297.5	------ .002243	6.19 ---	39.20 ---	39.80 ---	--- 20.5	Fluttered in first bending mode with $12\frac{1}{2}$-inch tip amplitude
34	None None	------ ------	0 331.5	0 0	0 .3040	0 1.341	0 343.5	------ .002219	6.43 ---	36.11 ---	45.94 ---	--- 22.1	Fluttered in second bending from 228 to 257 fps (indicated) and in first bending at 331.5 fps (indicated) with $\frac{1}{2}$-inch tip amplitude.
35	6 6	47 (tip) 47 (tip)	0 318.5	0 0	0 .2900	0 1.329	0 322	------ .002285	2.63 ---	31.96 ---	16.85 ---	--- 22.40	Fluttered in second bending mode with node at tip and $\frac{1}{2}$-inch amplitude at midspan.
36	6 6	41 41	0 374	0 0	0 .3476	0 1.540	0 388.5	------ .002216	3.33 ---	36.0 ---	17.82 ---	--- 0	No flutter; divergence
37	6 6	$36\frac{1}{2}$ $36\frac{1}{2}$	0 380	0 0	0 .3524	0 1.551	0 394	------ .002203	3.70 ---	36.47 ---	17.82 ---	--- 0	No flutter; divergence
38	6 6	29 29	0 369	0 0	0 .3412	0 1.487	0 384	------ .002188	4.46 ---	33.21 ---	17.78 ---	--- 0	No flutter; divergence
39	6 6	26 26	0 378	0 0	0 .3512	0 1.519	0 396	------ .002174	4.80 ---	31.36 ---	17.89 ---	--- 0	No flutter; divergence
40	6 6	21 21	0 387	0 0	0 .3590	0 1.549	0 405	------ .002168	5.44 ---	32.67 ---	17.82 ---	--- 28.1	Fluttered in first bending mode.

TABLE II.- EXPERIMENTAL DATA - Continued

Run	Weight	Spanwise position (in. from root)	V_1 (fps)	Percentage of Freon-12	Mach number	Reynolds number	V (fps)	ρ (slug/cu ft)	f_{h_1} (cps)	f_{h_2} (cps)	f_t (cps)	f_f (cps)	Remarks
41	6	11	318	0	0.2931	1.287×10^6	330.5	0.002211	---	---	---	16.8	Fluttered in first bending mode.
42	None		246	0	.2235	.9954	253	.002245	---	---	---	37.19	Fluttered in second bending from 220 to 250 fps
43	None	---	0	0	0	0	0	------	6.32	36.11	45.2	---	Fluttered in first bending mode with 8-inch amplitude; end plate installed in tunnel.
	None	---	311	0	.2846	1.217	326	.002168	---	---	---	21.78	
44	6	47 (tip)	288	0	.2831	1.123	301.5	.002168	---	---	---	21.97	Fluttered in first bending mode; end plate installed in tunnel
	6	47 (tip)	0	0	0	0	0	------	2.84	31.36	16.33	---	
	None	------	0	0	0	0	0	------	6.3	35.93	44.92	---	
45	6	47 (tip)	300	0	.2762	1.171	316	.002148	---	---	---	21.78	Fluttered in second bending mode; no end plate in tunnel.
	6	47 (tip)	0	0	0	0	0	------	2.85	30.63	16.33	---	
	6	47 (tip)	0	0	0	0	0	------	2.93	31.71	17.5	---	
	6	47 (tip)	0	0	0	0	0	------	2.88	31.63	16.90	---	
46	6	44	0	0	0	0	0	------	3.10	33.92	17.29	---	No flutter; divergence; end plate installed in tunnel
	6	44	312	0	.3249	1.429	365.2	.002206	---	---	---	0	
47	6	41	342	0	.3141	1.476	346.1	.002332	---	---	---	0	No flutter; divergence; end plate installed in tunnel.
	6	41	0	0	0	0	0	------	3.34	35.64	17.50	---	
48	6	$36\frac{1}{2}$	0	0	0	0	0	------	3.71	36.75	17.82	---	No flutter; divergence; end plate installed in tunnel.
	6	$36\frac{1}{2}$	346	0	.3167	1.480	349.6	.002322	---	---	---	0	
49	6	29	344	0	.3150	1.461	348.7	.002307	---	---	---	0	No flutter; divergence; end plate installed in tunnel.
	6	29	0	0	0	0	0	------	4.51	21.30	17.50	---	
50	6	26	0	0	0	0	0	------	4.84	30.95	17.42	---	No flutter; divergence; end plate installed in tunnel.
	6	26	349	0	.3186	1.472	353.3	.002300	---	---	---	0	
51	6	$20\frac{1}{2}$	0	0	0	0	0	------	5.51	Not clear	17.29	---	Fluttered with small amplitude; end plate installed in tunnel
	6	$20\frac{1}{2}$	344	0	.3151	1.453	349.8	.002295	---	---	---	24.50	
52	6	11	315	0	.2877	1.339	319.3	.002319	---	---	---	16.33	Fluttered with small amplitude; end plate installed in tunnel
	6	11	0	0	0	0	0	------	6.19	35.0	21.44	---	
53	6	11	324	0	.2961	1.499	328.7	.002321	---	---	---	16.55	Check on previous run; larger amplitude
54	7e	48 (tip)	0	0	0	0	0	------	3.00	27.4	21.44	---	Probably fluttered in first bending mode.
	7e	48 (tip)	337	0	.3101	1.431	338	.002303	---	---	---	8.85	
	7e	48 (tip)	0	0	0	0	0	------	3.01	28.00	21.76	---	
55	7e	40	0	0	0	0	0	------	3.58	34.59	22.7	---	Fluttered in first bending mode
	7e	40	310	0	.2824	1.313	314	.002318	---	---	---	11.43	
	7e	40	0	0	0	0	0	------	3.56	34.59	22.79	---	
56	7e	35	0	0	0	0	0	------	4.02	35.64	23.9	---	
	7e	35	292	0	.2658	1.241	295.5	.002327	---	---	---	13.0	
	7e	35	0	0	0	0	0	------	4.04	35.6	24.0	---	
57	7e	29	0	0	0	0	0	------	4.67	30.2	25.3	---	
	7e	29	294	0	.2680	1.246	298	.002321	---	---	---	14.52	
	7e	29	0	0	0	0	0	------	4.67	29.8	25.3	---	
58	7e	21	0	0	0	0	0	------	5.57	29.4	29.1	---	Small-amplitude flutter
	7e	21	283	0	.2569	1.201	286	.002332	---	---	---	17.6	
59	7e	11	308	0	.2810	1.297	312	.002324	---	---	---	23.33	Fluttered in first bending mode
	7e	11	0	0	0	0	0	------	6.28	26.7	37.4	---	
60	None		0	0	0	0	0	------	6.40	37.2	45.5	---	Fluttered in first bending modes; check on previous runs for unweighted wing
	None		330	0	.3020	1.385	338	.002292	---	---	---	22.0	
61	7d	48 (tip)	0	0	0	0	0	------	3.07	27.6	20.7	---	Fluttered in first bending mode; very close to divergence
	7d	48 (tip)	365	0	.3369	1.465	382	.002190	---	---	---	9.87	
	7d	48 (tip)	0	0	0	0	0	------	2.97	27.4	20.6	---	
	None	------	0	0	0	0	0	------	6.3	35.6	45.0	---	

TABLE II.- EXPERIMENTAL DATA - Continued

Run	Weight	Spanwise position (in. from root)	V_1 (fps)	Percentage of Freon-12	Mach number	Reynolds number	V (fps)	ρ (slug/cu ft)	f_{h_1} (cps)	f_{h_2} (cps)	f_t (cps)	f_f (cps)	Remarks
62	7d 7d 7d	44 44 44	0 367 0	0 0 0	0 .3390 0	0 1.465 $\times 10^6$ 0	0 384.4 0	--- 0.002179 ---	3.21 --- 3.21	30.3 --- 30.3	21.8 --- 21.4	--- 0 ---	No flutter; divergence
63	7d 7d 7d	39 39 39	0 350 0	0 0 0	0 .3220 0	0 1.388 0	0 365 0	--- .002175 ---	3.60 --- 3.59	34.4 --- 34.0	22.5 --- 22.4	--- 11.2 ---	Fluttered in first bending mode intermittently near top speed
64	7d 7d 7d	33 33 33	0 331 0	0 0 0	0 .3089 0	0 1.319 0	0 343 0	--- .00220 ---	4.2 --- 4.2	33.5 --- 33.0	24.1 --- 23.0	--- 13.2 ---	Fluttered in first bending mode with 2-inch tip amplitude
65	7d 7d 7d	27 27 27	0 319 0	0 0 0	0 .2916 0	0 1.274 0	0 331 0	--- .002206 ---	4.8 --- 4.78	27.4 --- 27.4	25.7 --- 25.6	--- 15.3 ---	Fluttered in first bending mode
66	7d 7d 7d	21 21 21	0 306 0	0 0 0	0 .2802 0	0 1.223 0	0 318 0	--- .002205 ---	5.4 --- 5.44	23.0 --- 23.3	26.2 --- 26.0	--- 17.6 ---	Fluttered in first bending mode
67	7d 7d 7d	11 11 11	0 308 0	0 0 0	0 .2811 0	0 1.230 0	0 320 0	--- .002210 ---	6.13 --- 6.05	24.0 --- 25.0	33.3 --- 33.2	--- 20.0 ---	Fluttered in second bending mode
68	7e 7e 7e	48 (tip) 48 (tip) 48 (tip)	0 370 0	0 0 0	0 .3422 0	0 1.504 0	0 384.6 0	--- .002206 ---	2.93 --- 2.99	28.0 --- 28.0	19.6 --- 20.0	--- 0 ---	No flutter; divergence
69	7e 7e 7e	44 44 44	0 362 0	0 0 0	0 .3339 0	0 1.458 0	0 376.6 0	--- .002196 ---	3.2 --- 3.19	30.4 --- 30.4	20.63 --- 20.4	--- 0 ---	No flutter; divergence
70	7e 7e 7e	40 40 40	0 352 0	0 0 0	0 .3237 0	0 1.411 0	0 366.1 0	--- .002196 ---	3.5 --- 3.5	33.79 --- 33.8	21.2 --- 21.19	--- 0 ---	No flutter; divergence
71	7e 7e 7e	34 34 34	0 366 0	0 0 0	0 .3377 0	0 1.450 0	0 383.0 0	--- .002163 ---	4.02 --- 4.02	34.6 --- 34.3	22.13 --- 22.13	--- 0 ---	No flutter; divergence
72	7e 7e 7e	28 28 28	0 346 0	0 0 0	0 .3187 0	0 1.365 0	0 364 0	--- .002167 ---	4.6 --- 4.66	29.4 --- 29.4	23.1 --- 23.1	--- 14.0 ---	Fluttered intermittently in first bending mode near top speed
73	7e 7e 7e	21 21 21	0 329 0	0 0 0	0 .3023 0	0 1.287 0	0 346 0	--- .002157 ---	5.39 --- 5.39	22.62 --- 22.4	26.0 --- 26.0	--- 16.5 ---	Fluttered in first bending mode
74	7e 7e 7e	11 11 11	0 310 0	0 0 0	0 .2842 0	0 1.208 0	0 326 0	--- .002157 ---	6.19 --- 6.12	26.63 --- 26.73	34.59 --- 34.43	--- 19.6 ---	Fluttered in first bending mode with 2-inch tip amplitude
75	7b 7b 7b	48 (tip) 48 (tip) 48 (tip)	0 331 0	0 0 0	0 .3047 0	0 1.281 0	0 349 0	--- .002135 ---	2.97 --- 2.95	28.82 --- 28.45	18.38 --- 18.15	--- 21.0 ---	Fluttered in second bending mode; clear response on record
76	7b 7b 7b	44 44 44	0 354 0	0 0 0	0 .3264 0	0 1.357 0	0 375.4 0	--- .002113 ---	3.19 --- 3.21	31.02 --- 30.95	19.22 --- 19.12	--- 0 ---	No flutter; divergence

TABLE II.- EXPERIMENTAL DATA - Concluded

Run	Weight	Spanwise position (in. from root)	V_i (fps)	Percentage of Freon-12	Mach number	Reynolds number	V (fps)	ρ (slug/cu ft)	f_{h_1} (cps)	f_{h_2} (cps)	f_t (cps)	f_f (cps)	Remarks
77	7b	38	0	0	0	0	0	- - - - -	3.70	35.0	20.1	- - -	No flutter; divergence
	7b	38	348	0	.3210	1.396 $\times 10^6$	369.5	0.002116	- - -	- - -	- - -	0	
	7b	38	0	0	0	0	0	- - - - -	3.68	34.6	20.28	- - -	
78	7b	28	0	0	0	0	0	- - - - -	4.67	29.4	21.0	- - -	No flutter; divergence
	7b	28	348	0	.3202	1.391	368.9	.002113	- - -	- - -	- - -	0	
	7b	28	0	0	0	0	0	- - - - -	4.67	29.4	21.3	- - -	
79	7b	21	0	0	0	0	0	- - - - -	5.33	25.0	98.0	- - -	Fluttered in second bending mode
	7b	21	348	0	.3200	1.383	370	.002105	- - -	- - -	- - -	24.5	
80	7b	11	307.5	0	.2818	1.179	325	.002128	- - -	- - -	- - -	18.54	Fluttered in first bending mode; clear response
	7b	11	0	0	0	0	0	- - - - -	6.12	25.57	33.6	- - -	
81	7f	48 (tip)	258	0	.2354	1.018	268.5	.002191	- - -	- - -	- - -	7.5	Fluttered in first bending mode with $\frac{1}{16}$-inch tip amplitude
	7f	48 (tip)	0	0	0	0	0	- - - - -	3.02	27.27	20.0	- - -	
82	7f	40	0	0	0	0	0	- - - - -	3.7	33.9	22.0	- - -	Fluttered in second bending mode with 1-inch amplitude
	7f	40	255	0	.2316	1.018	262.5	.002219	- - -	- - -	- - -	9.86	
	7f	40	0	0	0	0	0	- - - - -	3.65	34.3	22.0	- - -	
83	7f	32	0	0	0	0	0	- - - - -	4.36	33.3	21.0	- - -	Fluttered in second bending mode
	7f	32	237	0	.2160	.9474	246	.002218	- - -	- - -	- - -	12.0	
	7f	32	0	0	0	0	0	- - - - -	4.4	35.8	22.0	- - -	
84	7f	24	0	0	0	0	0	- - - - -	5.3	31.3	21.2	- - -	Fluttered in second bending mode
	7f	24	220	0	.2006	.8787	229	.002216	- - -	- - -	- - -	14.3	
	7f	24	0	0	0	0	0	- - - - -	5.2	32.4	31.0	- - -	
85	7f	16	0	0	0	0	0	- - - - -	6.0	35.3	34.6	- - -	Fluttered intermittently near top speed
	7f	16	243	0	.2212	.9634	252	.002205	- - -	- - -	- - -	17.15	
86	7f	11	0	0	0	0	0	- - - - -	6.2	38.2	34.3	- - -	Fluttered in first bending mode
	7f	11	267	0	.2437	1.011	278	.002185	- - -	- - -	- - -	19.1	
	7f	11	0	0	0	0	0	- - - - -	6.2	38.46	39.3	- - -	
87	7a	48 (tip)	0	0	0	0	0	- - - - -	2.41	29.6	Not clear	- - -	Fluttered in second bending mode with 1-inch amplitude; clear response
	7a	48 (tip)	306	0	.2790	1.173	320	.002135	- - -	- - -	- - -	21.4	
	7a	48 (tip)	0	0	0	0	0	- - - - -	3.0	30	Not clear	- - -	
88	7a	46	0	0	0	0	0	- - - - -	3.16	31.75	17.6	- - -	Fluttered in second bending mode with strong clear response
	7a	46	345	0	.3194	1.316	358	.002099	- - -	- - -	- - -	21.8	
89	7a	47	0	0	0	0	0	- - - - -	3.06	30.0	Not clear	- - -	Fluttered in second bending mode; clear response; possibly two modes visible
	7a	47	319	0	.2939	1.217	339.2	.002109	- - -	- - -	- - -	21.6	
90	7a	45	0	0	0	0	0	- - - - -	2.12	31.4	18.0	- - -	No flutter; divergence
	7a	45	358	0	.3314	1.344	382.8	.002077	- - -	- - -	- - -	0	
91	7a	8	0	0	0	0	0	- - - - -	6.2	36.0	27.0	- - -	Fluttered in first bending mode
	7a	8	304	0	.2794	1.152	323.3	.002102	- - -	- - -	- - -	19.1	
92	7a	11	0	0	0	0	0	- - - - -	6.1	33.6	22.5	- - -	Fluttered in first bending mode
	7a	11	304	0	.2794	1.147	323.5	.002097	- - -	- - -	- - -	17.4	
	7a	11	0	0	0	0	0	- - - - -	6.3	34.5	23.1	- - -	
93	7a	14	0	0	0	0	0	- - - - -	6.05	Not clear	20.6	- - -	Fluttered in first bending mode
	7a	14	321	0	.2956	1.213	342.3	.002093	- - -	- - -	- - -	16.3	
94	7a	17	0	0	0	0	0	- - - - -	5.9	Not clear	19.7	- - -	Flutter debatable; looked closer to divergence
	7a	17	336	0	.3294	1.531	381.8	.002062	- - -	- - -	- - -	16.9	
95	7a	16	0	0	0	0	0	- - - - -	5.85	Not clear	20.0	- - -	Fluttered in first bending mode
	7a	16	351	0	.3239	1.313	373.7	.002068	- - -	- - -	- - -	15.5	
	7a	16	0	0	0	0	0	- - - - -	6.0	30.6	18.5	- - -	
96	None	- - - - -	313	0	.2878	1.179	333.8	.002090	- - -	- - -	- - -	22.1	Fluttered in first bending mode
	None	- - - - -	0	0	0	0	0	- - - - -	6.25	36.8	44.6	- - -	

NACA

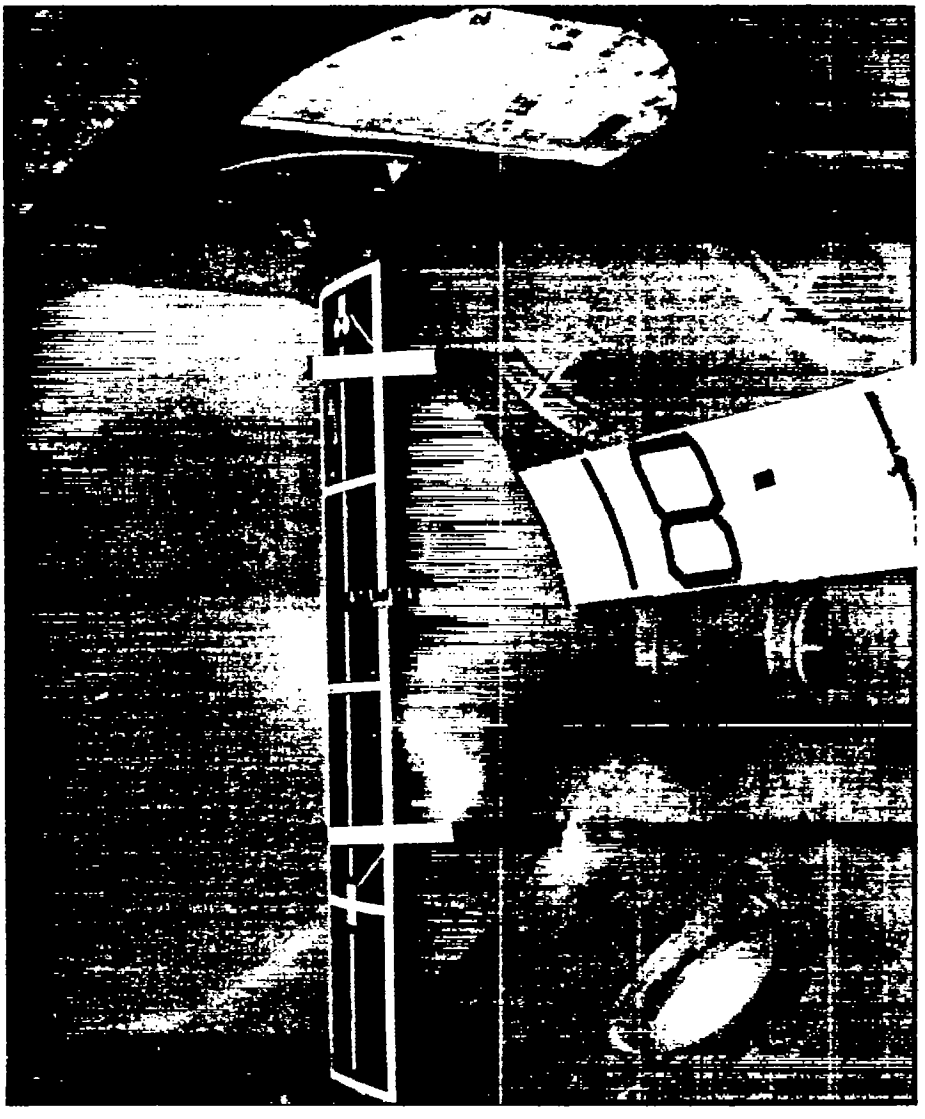

Figure 1.- General view of test section and model showing strain-gage locations.

L-53813

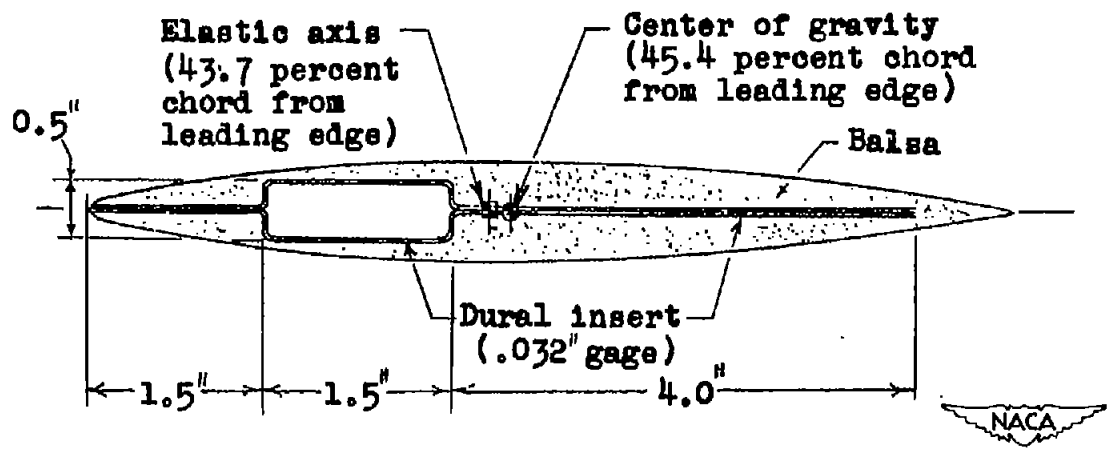

Figure 2.- Cross-sectional view of model.

(a) Weight 1.

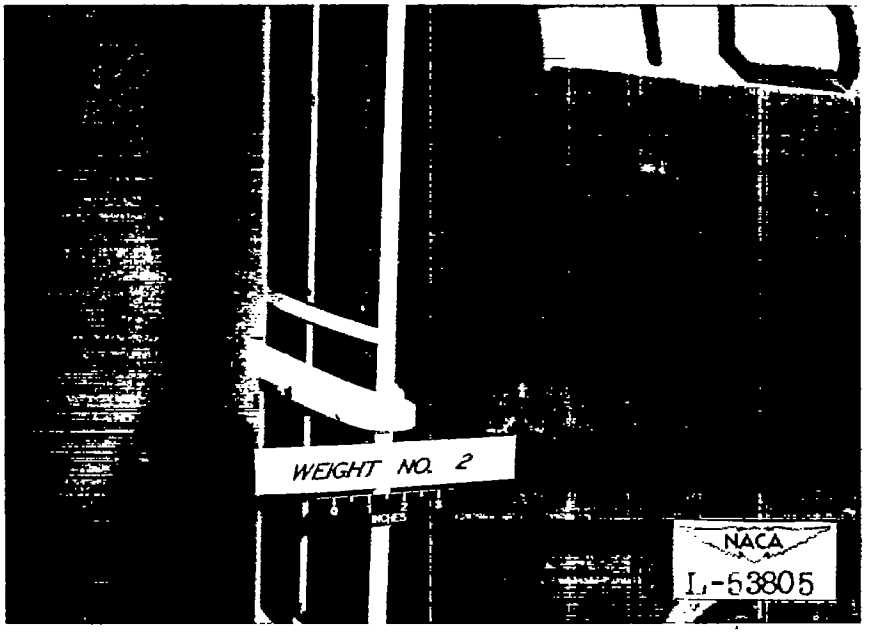

(b) Weight 2.

Figure 3.- Concentrated weights.

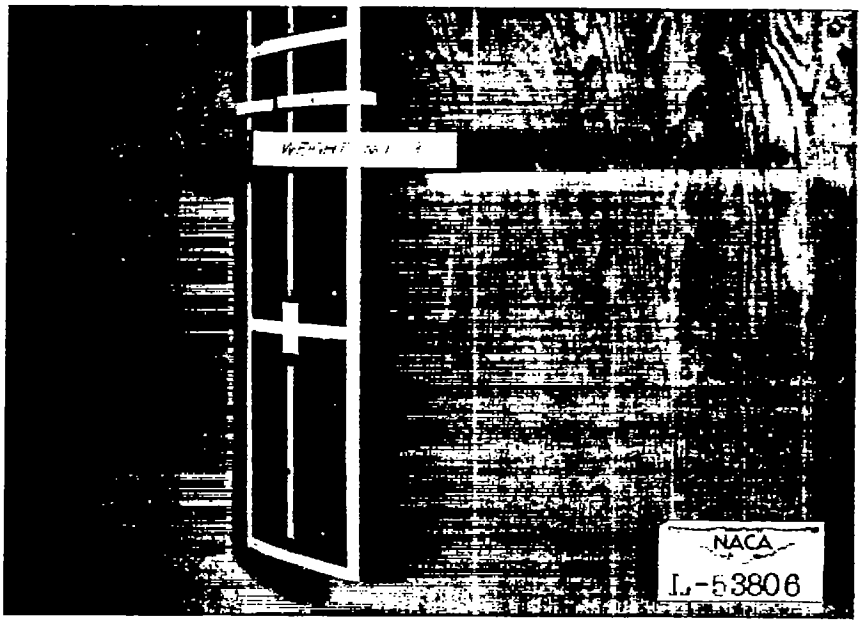

(c) Weight 3.

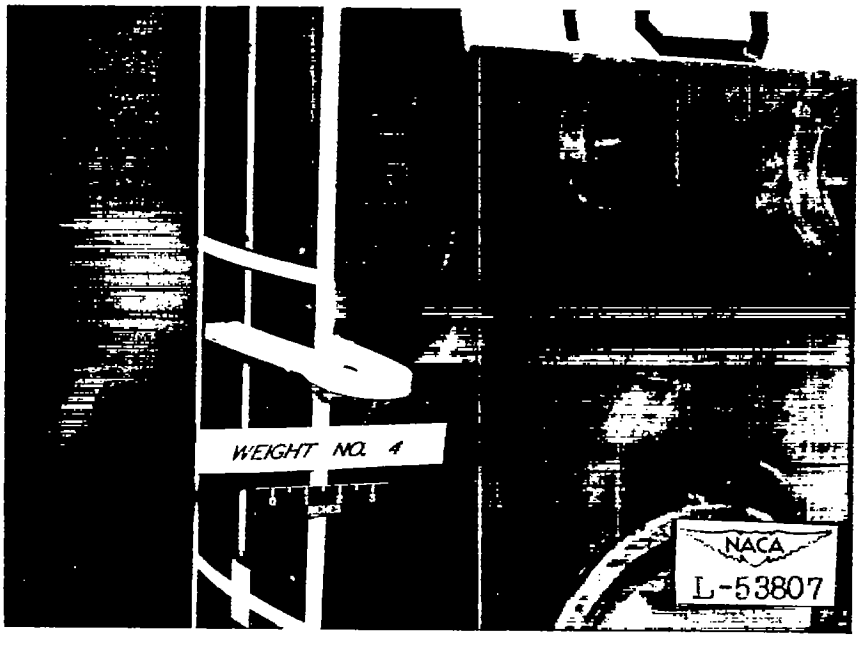

(d) Weight 4.

Figure 3.- Continued.

(e) Weight 5.

(f) Weight 6.

Figure 3.- Continued.

(g) Weight 7a.

Figure 3.- Concluded.

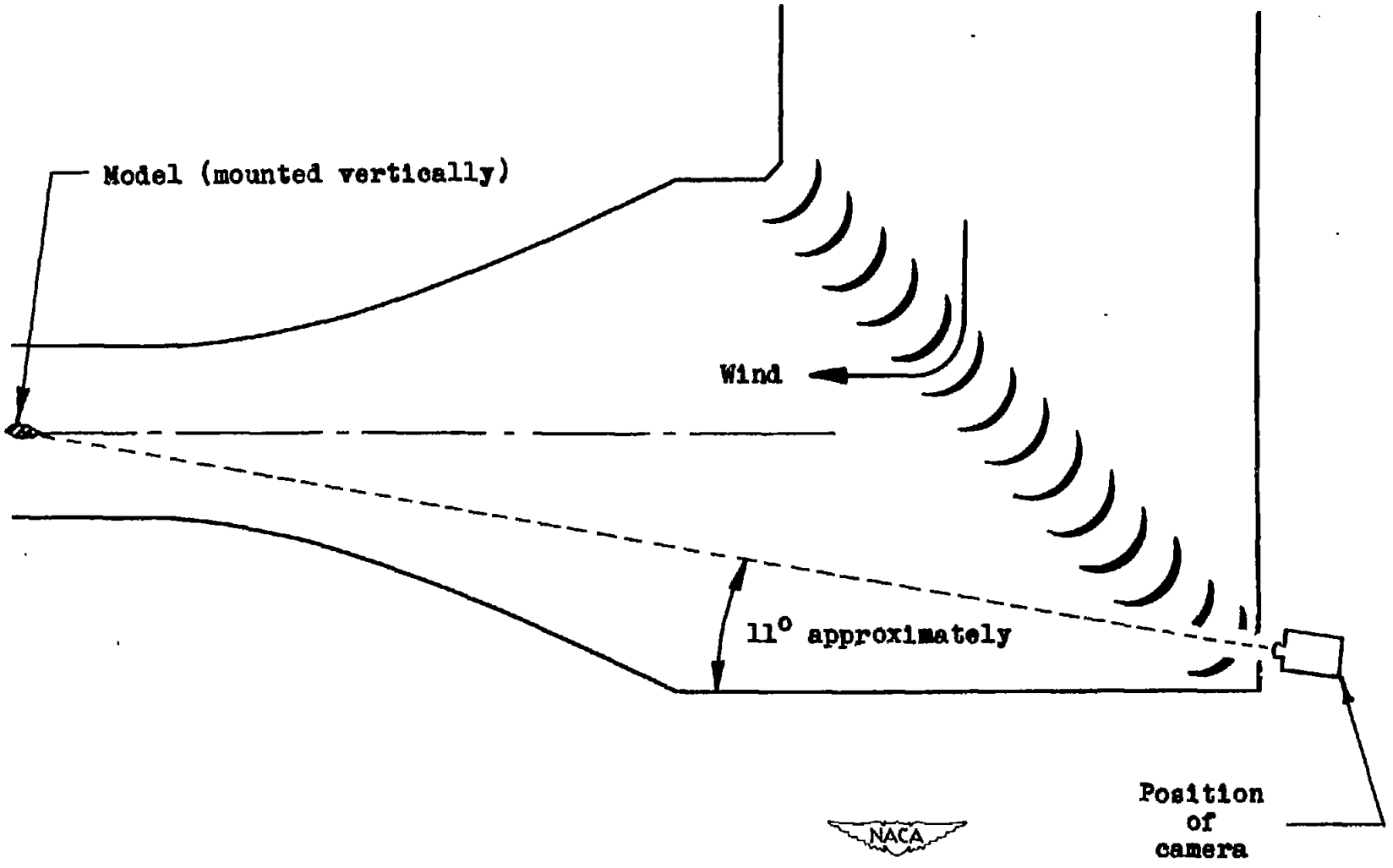

Figure 4.- Plan view of Langley 4.5-foot flutter-research tunnel showing camera location relative to test section.

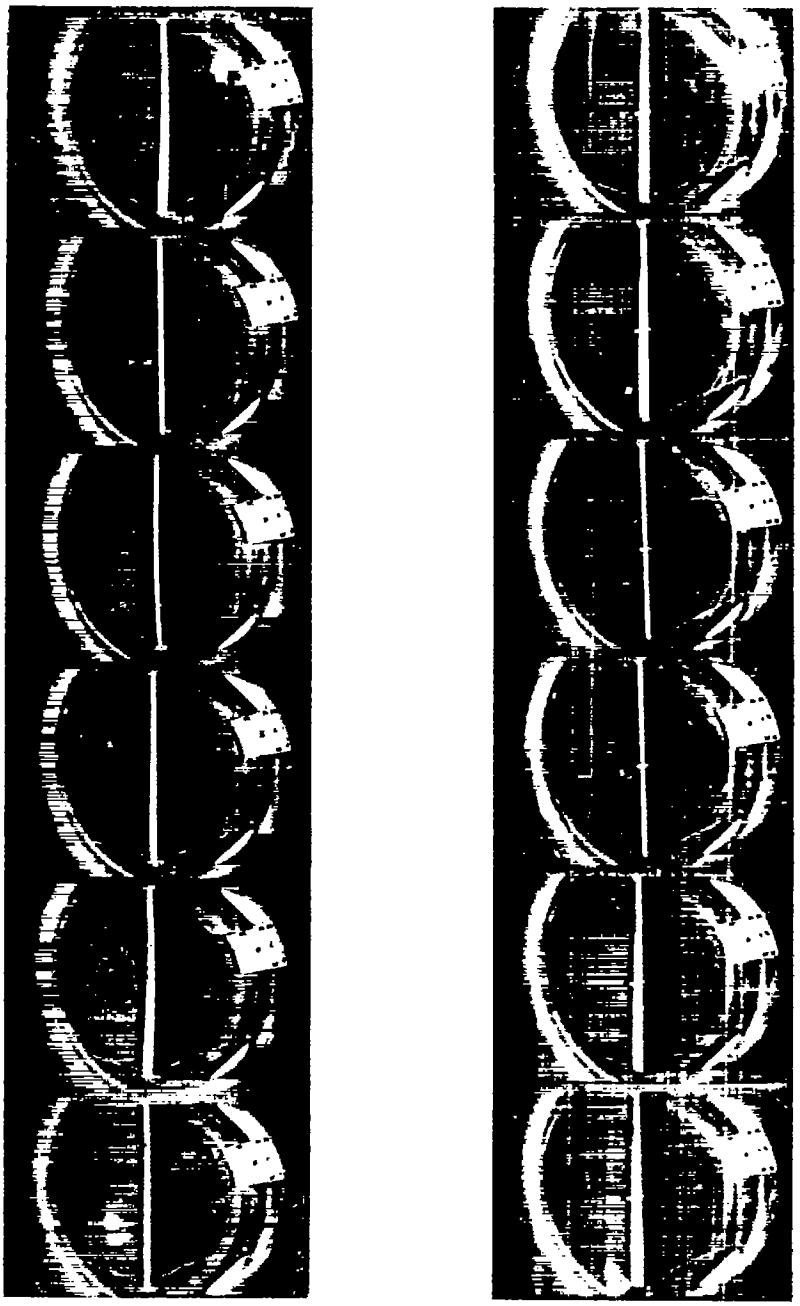

(a) Run 35. (b) Run 31.

Figure 5.- Motion-picture records of one cycle of flutter for different weight positions.

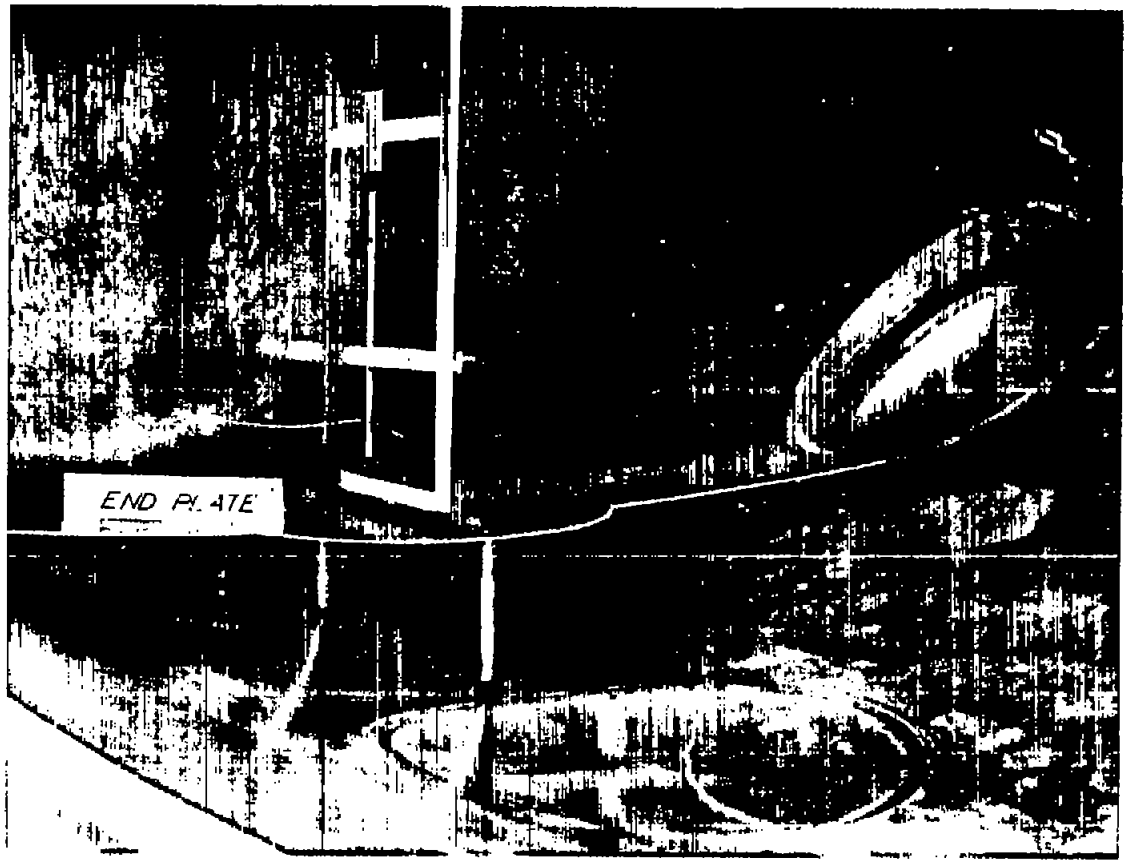

Figure 6.- End-plate installation. Note restraining wires for protecting model from destructive divergence.

NACA

L-53814

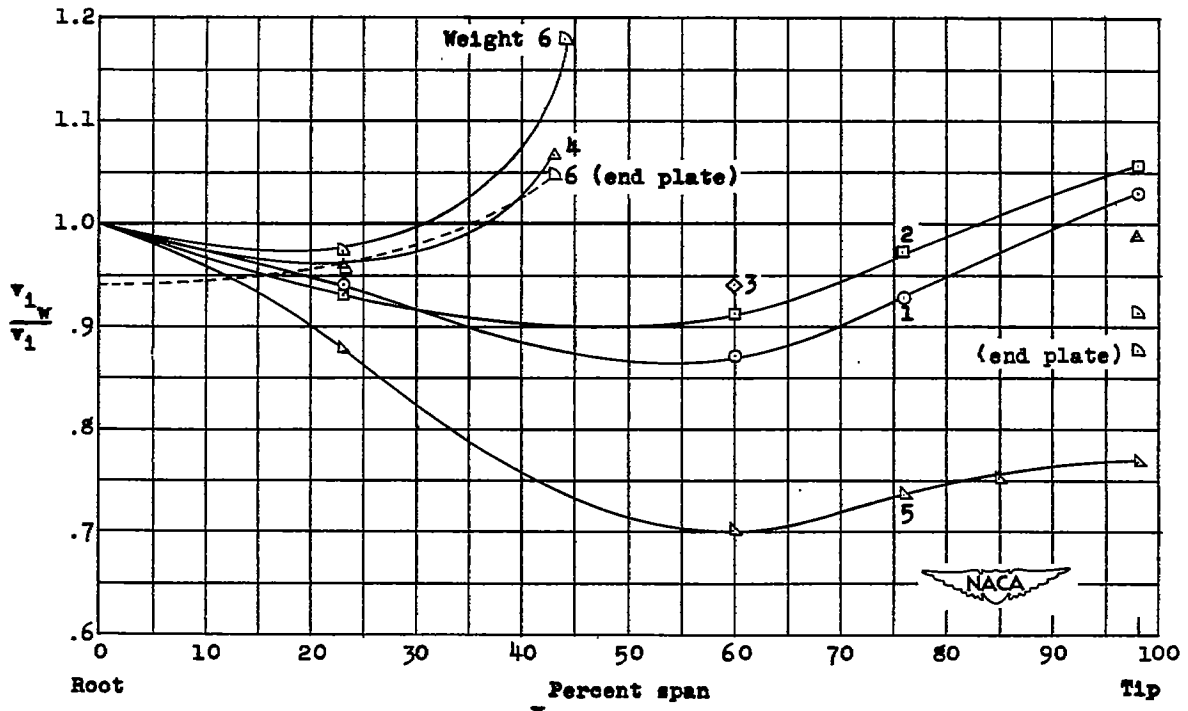

Figure 7.- Flutter-speed ratio $\frac{V_{i_W}}{V_i}$ against span position for weights 1 to 6.

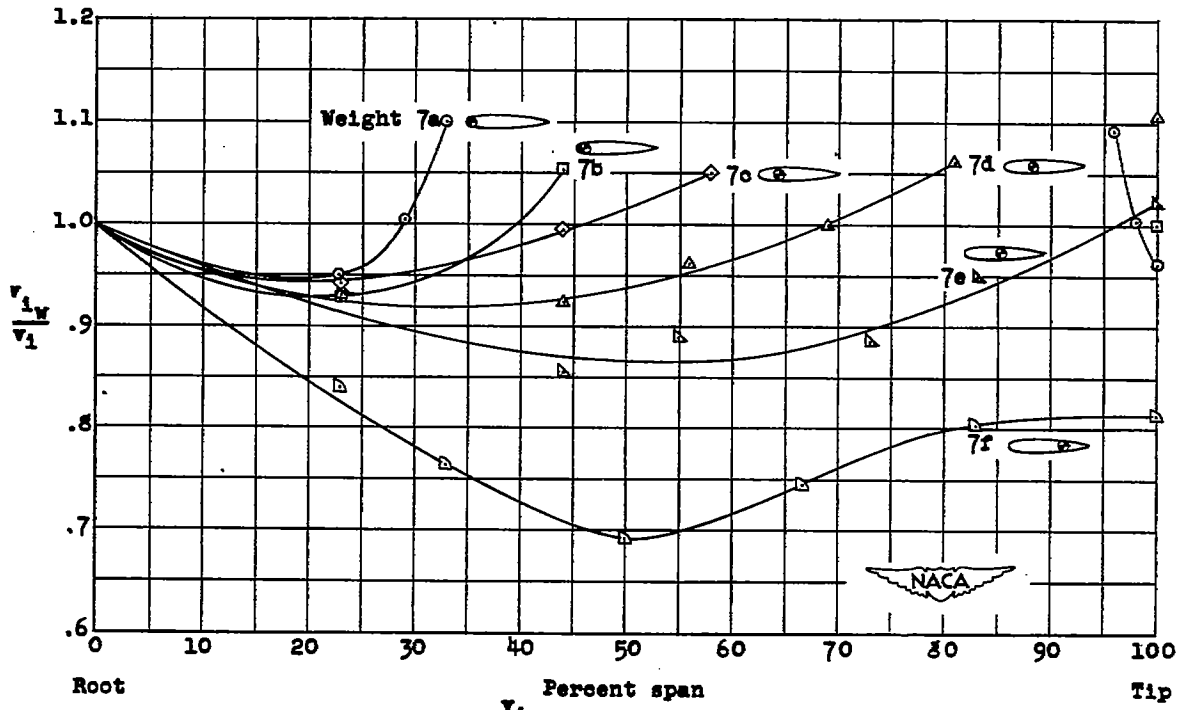

Figure 8.- Flutter-speed ratio $\frac{V_{i_W}}{V_i}$ against span position for weights 7a to 7f.

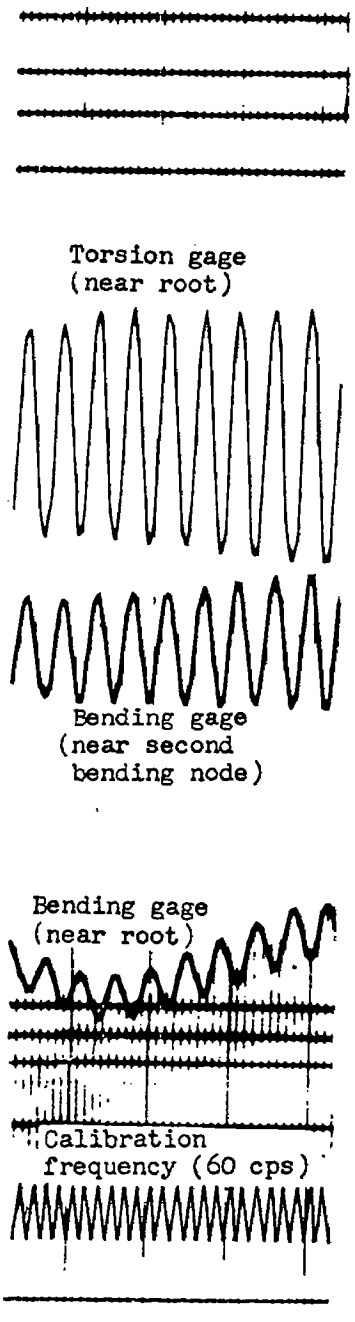

Figure 9.- Flutter record with weight 6 at tip and end plate in tunnel.

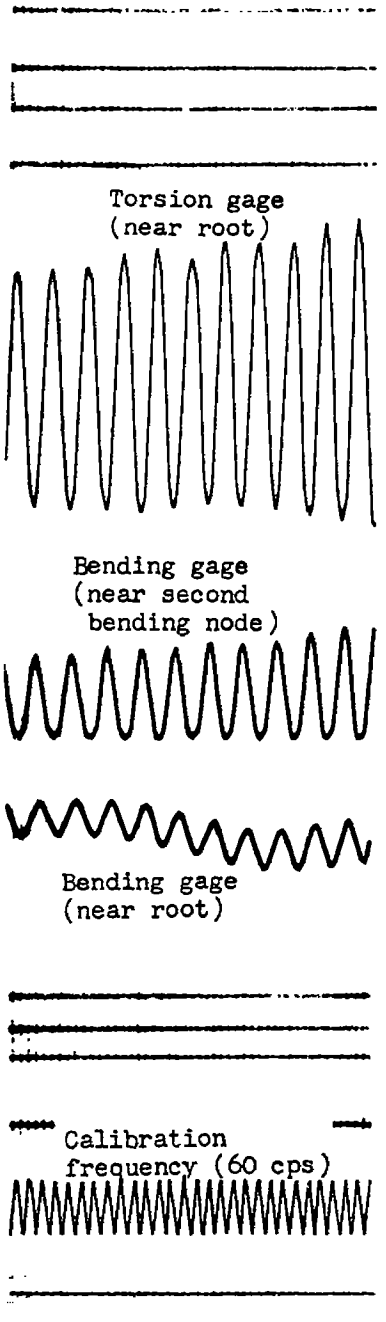

Figure 10.- Flutter record with weight 6 at tip without end plate in tunnel.

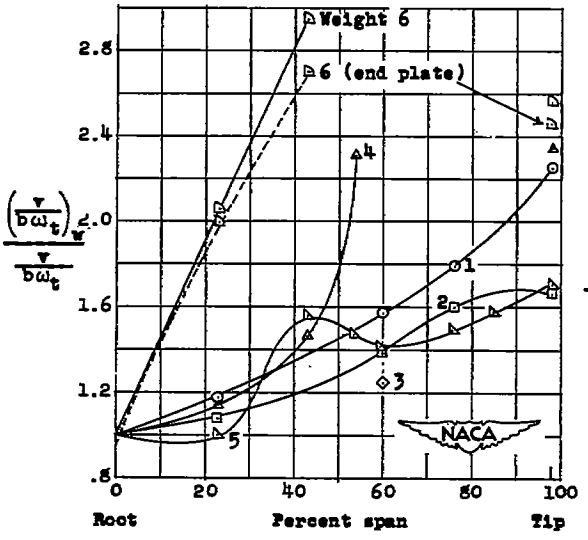

Figure 11.- Flutter-velocity-coefficient ratio against span position for weights 1 to 6.

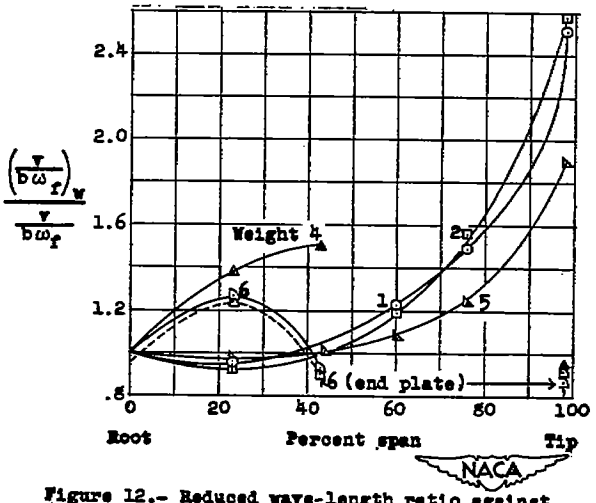

Figure 12.- Reduced wave-length ratio against span position for weights 1 to 6.

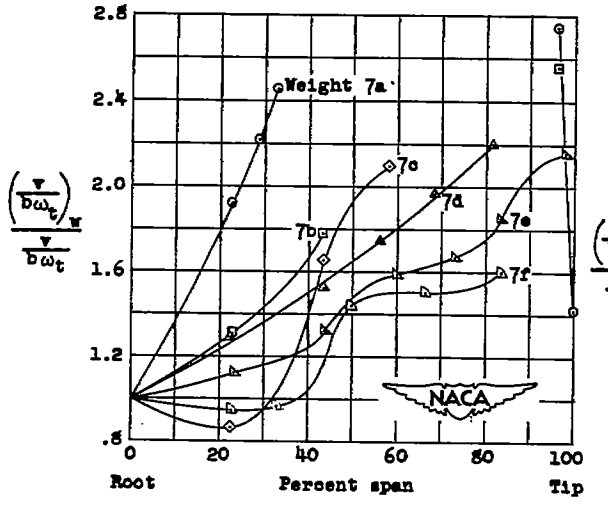

Figure 13.- Flutter-velocity-coefficient ratio against span position for weights 7a to 7f.

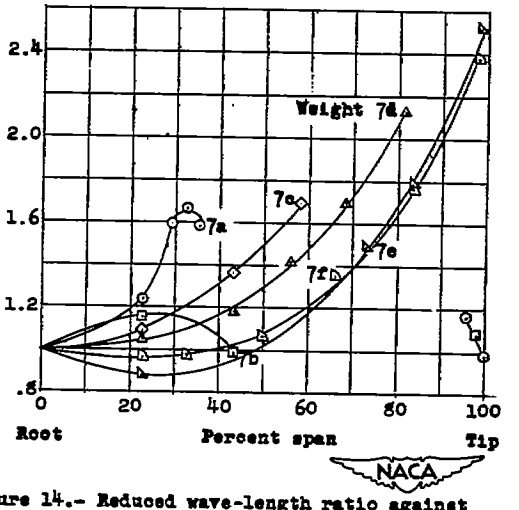

Figure 14.- Reduced wave-length ratio against span position for weights 7a to 7f.

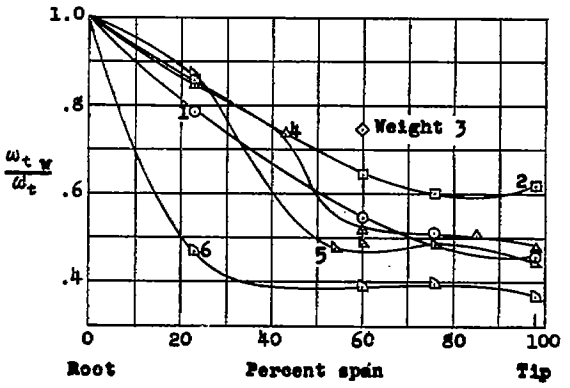

Figure 15.- Natural first torsional-frequency ratio $\frac{\omega_{t_W}}{\omega_t}$ against span position for weights 1 to 6.

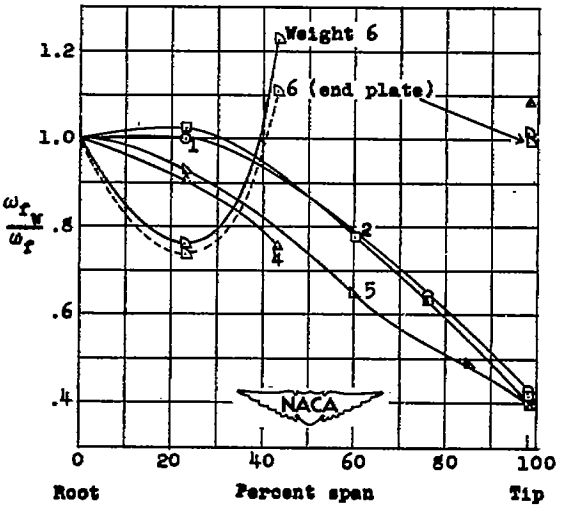

Figure 16.- Flutter-frequency ratio $\frac{\omega_{f_W}}{\omega_f}$ against span position for weights 1 to 6.

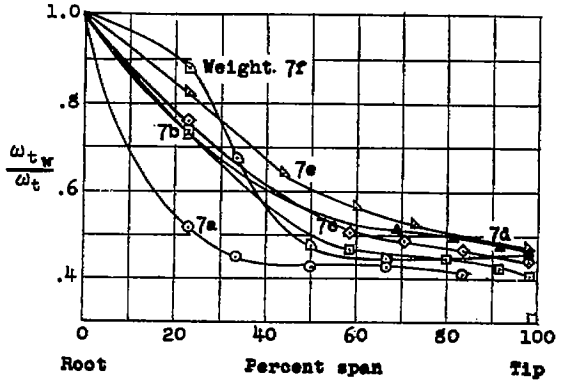

Figure 17.- Natural first torsional-frequency ratio $\frac{\omega_{t_W}}{\omega_t}$ against span position for weights 7a to 7f.

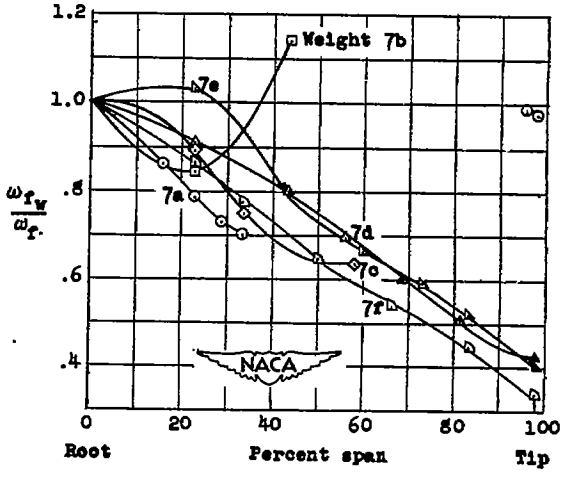

Figure 18.- Flutter-frequency ratio $\frac{\omega_{f_W}}{\omega_f}$ against span position for weights 7a to 7f.

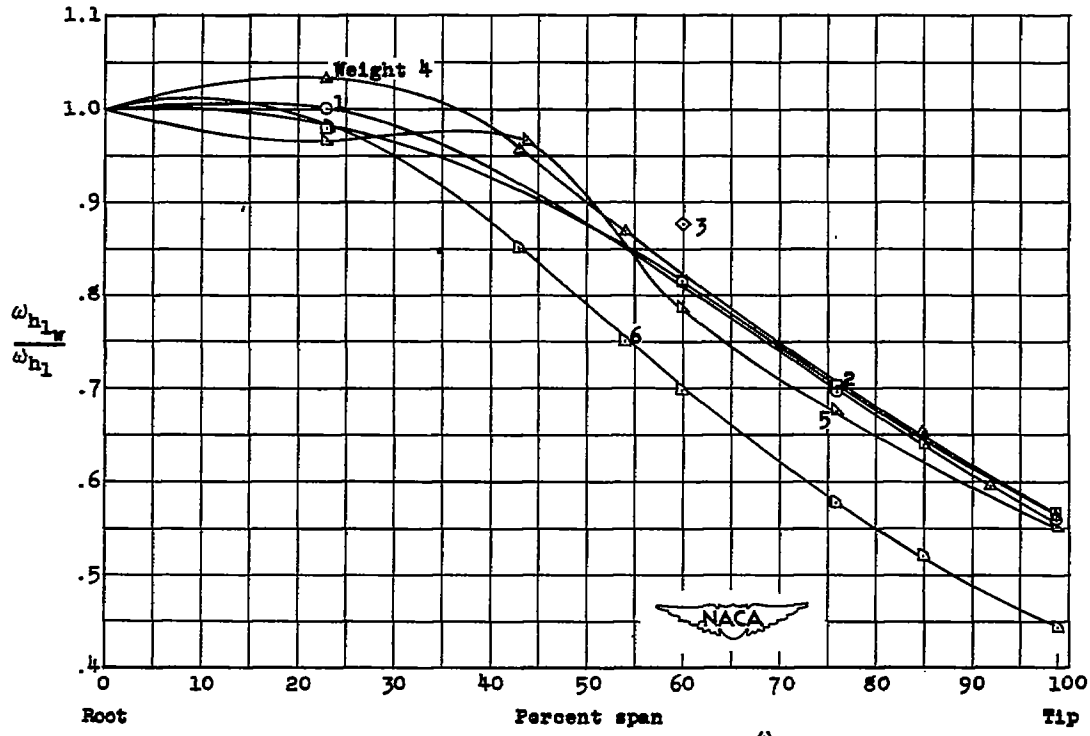

Figure 19.- Natural first-bending-frequency ratio $\frac{\omega_{h_{1_W}}}{\omega_{h_1}}$ against spar position for weights 1 to 6.

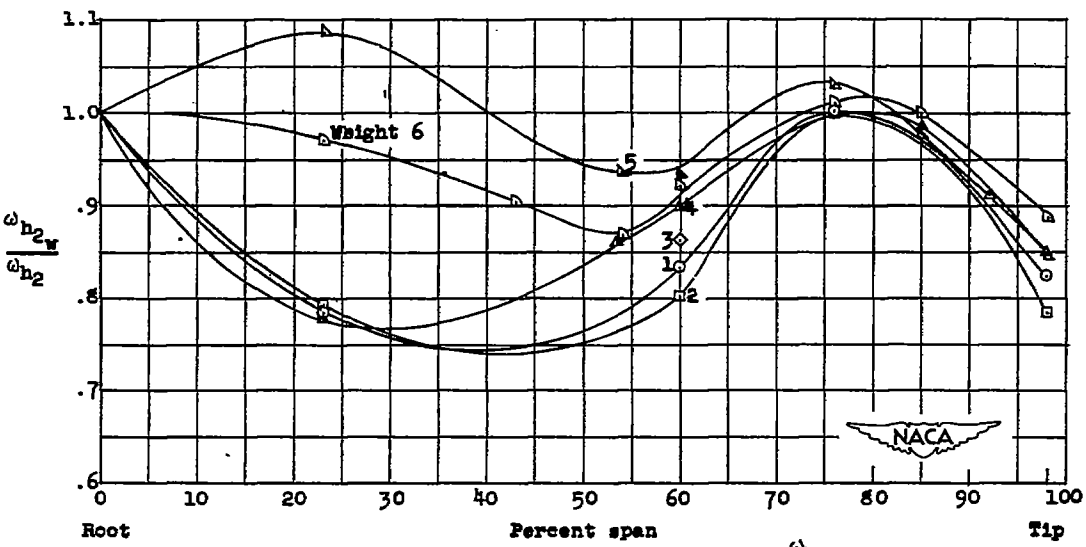

Figure 20.- Natural second-bending-frequency ratio $\frac{\omega_{h_{2_W}}}{\omega_{h_2}}$ against span position for weights 1 to 6.

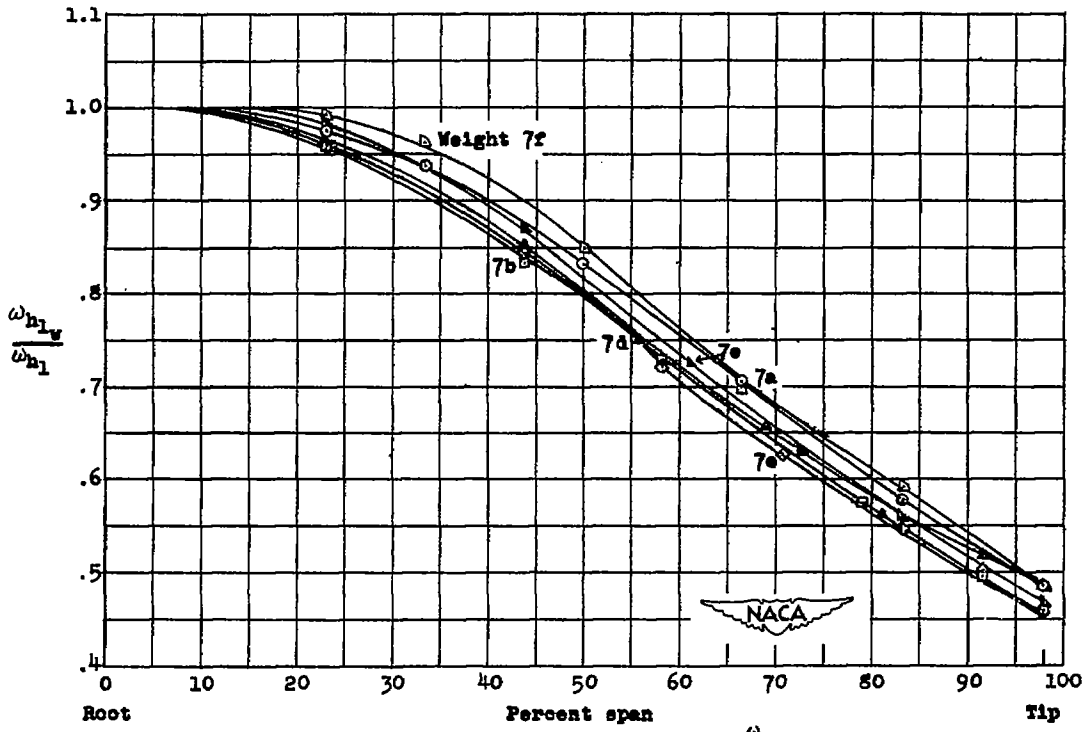

Figure 21.- Natural first-bending-frequency ratio $\frac{\omega_{h_{1_W}}}{\omega_{h_1}}$ against span position for weights 7a to 7f.

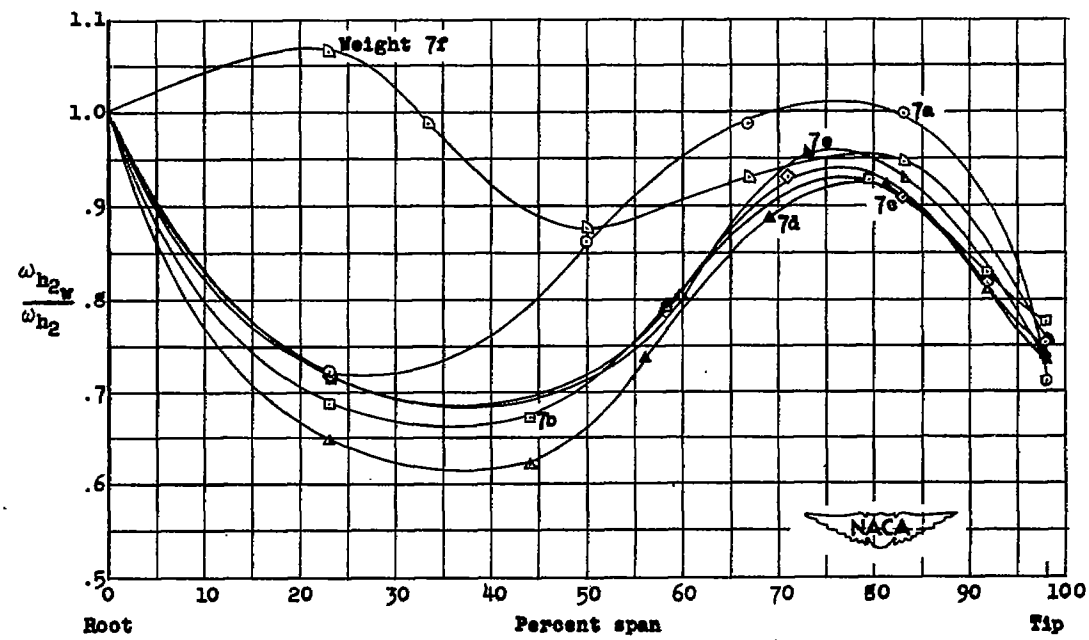

Figure 22.- Natural second-bending-frequency ratio $\frac{\omega_{h_{2_W}}}{\omega_{h_2}}$ against span position for weights 7a to 7f.

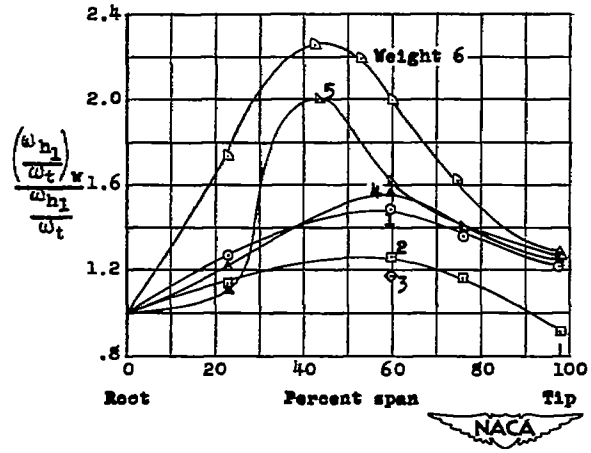

Figure 23.- Natural first-bending to first-torsional frequency ratio against span position for weights 1 to 6.

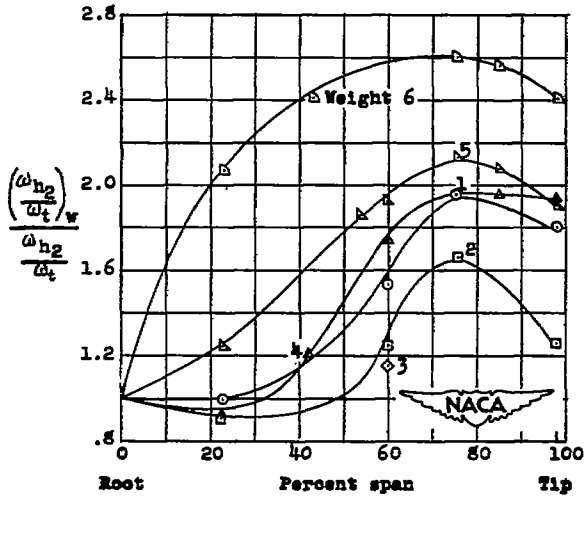

Figure 24.- Natural second-bending to first-torsional frequency ratio against span position for weights 1 to 6.

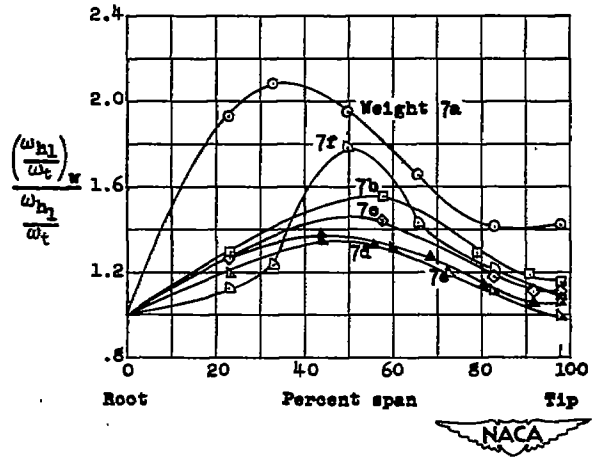

Figure 25.- Natural first-bending to first-torsional frequency ratio against span position for weights 7a to 7f.

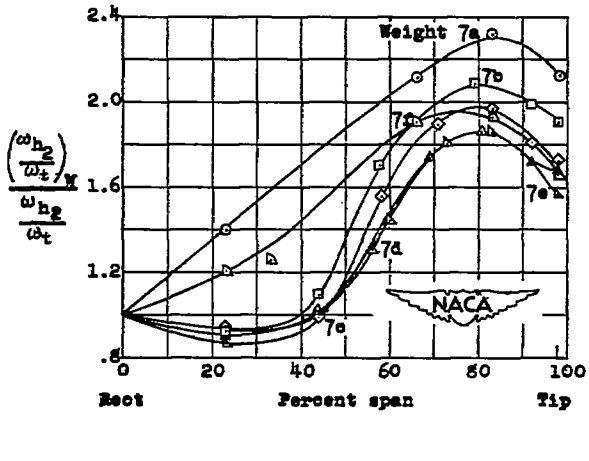

Figure 26.- Natural second-bending to first-torsional frequency ratio against span position for weights 7a to 7f.